

# On the Solubility of Three Disperse Anthraquinone Dyes in Supercritical Carbon Dioxide: New Experimental Data and Correlation

Jose P. Coelho,<sup>†,\*</sup> Andrea F. Mendonça,<sup>†</sup> António F. Palavra,<sup>‡</sup> and Roumiana P. Stateva<sup>§</sup>

<sup>†</sup>ISEL, DEQ, Chemical Engineering and Biotechnology Research Center, Rua Conselheiro Emídio Navarro, 1, 1959-007 Lisboa, Portugal

<sup>‡</sup>Complexo I, Centro de Química Estrutural, IST, Av. Rovisco Pais, 1096-001 Lisboa, Portugal

<sup>§</sup>Institute of Chemical Engineering, Bulgarian Academy of Sciences, Sofia 1113, Bulgaria

**ABSTRACT:** Solubility measurements of quinizarin (1,4-dihydroxyanthraquinone), disperse red 9 (1-(methylamino) anthraquinone), and disperse blue 14 (1,4-bis(methylamino)anthraquinone) in supercritical carbon dioxide (SC CO<sub>2</sub>) were carried out in a flow type apparatus, at a temperature range from (333.2 to 393.2) K and at pressures from (12.0 to 40.0) MPa. Mole fraction solubility of the three dyes decreases in the order quinizarin ( $2.9 \times 10^{-6}$  to  $2.9 \cdot 10^{-4}$ ), red 9 ( $1.4 \times 10^{-6}$  to  $3.2 \times 10^{-4}$ ), and blue 14 ( $7.8 \times 10^{-8}$  to  $2.2 \times 10^{-5}$ ). Four semiempirical density-based models were used to correlate the solubility of the dyes in the SC CO<sub>2</sub>. From the correlation results, the total heat of reaction, heat of vaporization plus the heat of solvation of the solute, were calculated and compared with the results presented in the literature. The solubilities of the three dyes were correlated also applying the Soave–Redlich–Kwong cubic equation of state (SRK CEoS) with classical mixing rules, and the physical properties required for the modeling were estimated and reported.

## 1. INTRODUCTION

Supercritical carbon dioxide (SC CO<sub>2</sub>) is an alternative benign solvent that is being considered in the textile industry for dry dyeing processes. The latter are an appealing green processing technique without wastewater emission and have received considerable attention because of increased environmental concerns.<sup>1–3</sup> Supercritical dyeing of textiles was originally developed for the dyeing of some synthetic polymers using mainly disperse dyes but has also been tested with natural fibres and different classes of dyes.<sup>4</sup>

The design, optimization, and application of supercritical dyeing processes require knowledge of the phase equilibrium involving dyes and the supercritical solvent. The solubility of eight disperse dyes, limited to a single temperature (80 °C) and to a small range of pressures, was reported by Ozcan et al.<sup>5</sup> Other authors studied the solubility of disperse anthraquinones and azo dyes in SC CO<sub>2</sub> and demonstrated that the solubility of the former are higher.<sup>6–18</sup> The methods employed by the investigators to recover the solutes differ considerably. This we believe can explain, to a certain extent, the errors and deviations of the solubility data reported in literature.

The goal of our work is to report new experimental data for the solubility of quinizarin (1,4-dihydroxyanthraquinone), disperse red 9 (1-(methylamino)anthraquinone), and disperse blue 14 (1,4-Bis(methylamino) anthraquinone) in SC CO<sub>2</sub> measured in a consistent and adequate range of pressures and temperatures and to thereby evaluate and compare it against the data published in the literature. These measurements were carried out over the temperature range (333 to 393) K and at pressures ranging from (12 to 40) MPa.

We have chosen to measure and correlate the solubility of the three dyes at these conditions because although there are a number of experimental measurements already reported by other

authors,<sup>19–23</sup> still, as will be briefly discussed hereunder, the latter are often in significant disagreement.

For example, for the dye, red 9,<sup>21,22</sup> the differences in the solubility values reported are as high as 200%. The deviations among the different data sets for blue 14<sup>21–23</sup> are also in a similar range. Hence, new sets of experimental data are needed to corroborate the viability of the existing data.

Two types of models were applied to correlate the solubilities of the dyes in SC CO<sub>2</sub>: namely, Chrastil model,<sup>24</sup> Bartle model,<sup>25</sup> Mendez-Santiago and Teja (M–T) model,<sup>26</sup> and Kumar and Johnson (K–J) model,<sup>27</sup> as well as the Soave–Redlich–Kwong cubic equation of state (SRK CEoS) with the one-fluid van der Waals mixing rule.<sup>28</sup> Furthermore, the total heat of reaction ( $\Delta H_{\text{total}}$ ), the heat of vaporization plus the heat of solvation of the solute were determined from the correlation results using the semiempirical equations and compared with the results available in the literature.

## 2. EXPERIMENTAL SECTION

**2.1. Chemicals.** High purity CO<sub>2</sub> (99.995% purity) was supplied by Air Liquide (Portugal). Quinizarin (>98 mass %), disperse red 9 (>98 mass %) and disperse blue 14 (>97 mass %) were purchased from Sigma Aldrich (Germany) and were used without further purification. The structures and the melting temperatures of the pure components are listed in Table 1.

**2.2. Experimental Apparatus and Procedures.** The supercritical fluid extraction experiments were performed in a flow

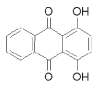
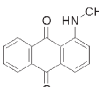
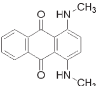
**Received:** July 6, 2010

**Accepted:** March 10, 2011

**Revised:** January 21, 2011

**Published:** March 18, 2011

**Table 1. Structure, Molar Mass, and Melting Temperature (According to the Supplier) for the Three Dyes**

Name	Structure	Empirical Formula (Molar mass)	Melting Point
1,4-Dihydroxyanthraquinone (Commercial name, Quinizarin)		C <sub>14</sub> H <sub>8</sub> O <sub>4</sub> (240.21 g/mol)	(468.15 to 473.15) K
1-(Methylamino) anthraquinone (Commercial name, Red 9)		C <sub>15</sub> H <sub>11</sub> NO <sub>2</sub> (237.25 g/mol)	(443.15 to 445.15) K
1,4-Bis(methylamino) anthraquinone (Commercial name, Blue 14)		C <sub>16</sub> H <sub>14</sub> N <sub>2</sub> O <sub>2</sub> (266.29 g/mol)	(493.15 to 495.15) K

through apparatus. A detailed description of the equipment has been reported previously.<sup>29,30</sup> This equipment permits carrying studies at temperatures up to 393.2 K and pressures up to 60.0 MPa. The uncertainties of the temperature and pressure measurements were  $\pm 1$  °C and  $\pm 1$  bar, respectively. The total volume of CO<sub>2</sub> was determined with a mass flow meter and a totalizer from Alicat Scientific (USA), model M-5 SLPM-D. The uncertainty associated with volume measurements was  $\pm 0.5\%$  in the total volume.

The equilibrium cell (volume of 50 mL) was built from AISI 316 stainless steel tubing (32 cm long and an ID of 1.41 cm). Inside the extractor approximately (3.5–4) g of dye is charged mixed with glass spheres of (0.71–1.18) mm in diameter, resulting in an overall bed height of about (15–18) cm. The conditions for the solubility studies were as follows: CO<sub>2</sub> flow rates of  $9.5 \times 10^{-3}$  g·s<sup>-1</sup> (linear velocity of  $8.7 \times 10^{-3}$  cm·s<sup>-1</sup>, contact time of solvent–solute, 1950 s), pressures up to 40.0 MPa and temperatures from (313.2–393.2) K. The flow rate of the supercritical fluid through the equilibrium cell was checked to verify the different contact times, from (640–2300) s for measurements of equilibrium solubilities, to ensure the saturation of the compound in the supercritical phase. Glass wool, before and after the packed bed, respectively, guarantees a uniform flow distribution and prevents dye particle entrainment. The extractor inlet and outlet are also provided with a 5  $\mu$ m filter disk.

The dyes were collected using an ice bath in a tube with three filters to make certain that the last filter was not colored. The three-way valve assures that at the end of the run the expansion valve, connecting lines and the three filters in the tube were washed with an appropriated organic solvent (e.g., methanol) to a fixed volume to guarantee a complete recovery of the dye. After each measurement, the system of filters was disconnected from the supercritical apparatus and replaced by a new one. The total amount of the dye collected was quantified by visible spectroscopy.

Careful cleanup for the supercritical equipment was used as we went from one dye to the other; namely, after an appropriated organic solvent had been used to wash all the lines and the equilibrium cell, a run with the empty system at 50.0 MPa, with a mixture of SC CO<sub>2</sub> and 10% methanol, was performed to guarantee the complete cleaning of the device.

**Table 2. Solubility,  $y_2$ , for Quinizarin, Red 9 and Blue 14<sup>a, b</sup> in SC CO<sub>2</sub> (1) from  $T = (333.2–393.2)$  K**

T/K	P (MPa)	quinizarin	red 9	blue 14	$\rho_1$ (kg m <sup>-3</sup> )
		10 <sup>6</sup> $y_2$	10 <sup>6</sup> $y_2$	10 <sup>6</sup> $y_2$	
333.2	12.0	4.64 $\pm$ 0.2	4.75 $\pm$ 0.2	0.195 $\pm$ 0.01	434.43
	15.0	25.8 $\pm$ 2	19.7 $\pm$ 0.2	1.01 $\pm$ 0.01	604.09
	20.0	57.9 $\pm$ 2	51.0 $\pm$ 1	2.46 $\pm$ 0.1	723.68
	22.5			3.46 $\pm$ 0.01	758.69
	25.0	83.0 $\pm$ 3	76.1 $\pm$ 1	4.27 $\pm$ 0.2	786.55
	30.0	113 $\pm$ 5	97.6 $\pm$ 2	5.54 $\pm$ 0.2	829.71
	35.0	143 $\pm$ 2	117 $\pm$ 4	7.18 $\pm$ 0.4	862.94
	40.0	163 $\pm$ 3	137 $\pm$ 2	8.02 $\pm$ 0.2	890.14
353.2	12.0	2.92 $\pm$ 0.1	1.43 $\pm$ 0.1	0.078 $\pm$ 0.003	296.74
	15.0	11.1 $\pm$ 0.3	7.87 $\pm$ 0.1	0.385 $\pm$ 0.005	427.15
	20.0	52.6 $\pm$ 0.5	44.8 $\pm$ 2	2.37 $\pm$ 0.2	593.89
	22.5	81.5 $\pm$ 0.5	73.4 $\pm$ 1	4.08 $\pm$ 0.1	646.04
	25.0	108 $\pm$ 4	98.4 $\pm$ 0.2	5.79 $\pm$ 0.2	686.22
	30.0	163 $\pm$ 7	147 $\pm$ 3	9.41 $\pm$ 0.4	745.60
	35.0	231 $\pm$ 10	196 $\pm$ 3	13.1 $\pm$ 0.2	788.97
	40.0			16.3 $\pm$ 0.6	823.18
373.2	12.0	3.27 $\pm$ 0.1	1.89 $\pm$ 0.09	0.111 $\pm$ 0.003	242.07
	15.0	10.0 $\pm$ 0.2	6.63 $\pm$ 0.3	0.441 $\pm$ 0.02	332.35
	20.0	49.4 $\pm$ 2.0	43.2 $\pm$ 2.0	2.64 $\pm$ 0.08	480.53
	22.5	77.0 $\pm$ 1.6	74.5 $\pm$ 2.0	4.87 $\pm$ 0.02	539.89
	25.0	112 $\pm$ 5	117 $\pm$ 3	7.76 $\pm$ 0.23	588.45
	30.0	200 $\pm$ 7	203 $\pm$ 4	15.1 $\pm$ 0.4	661.87
	35.0	289 $\pm$ 15	316 $\pm$ 13	21.6 $\pm$ 1.0	715.26
393.2	12.0	6.95 $\pm$ 0.39			210.31
	15.0	19.0 $\pm$ 0.6			280.36
	20.0	64.3 $\pm$ 3.0			401.15
	22.5	107 $\pm$ 2.0			456.45
	25.0	172 $\pm$ 2.0			505.56
	30.0	267 $\pm$ 5			585.22

<sup>a</sup> Average values of mole fraction taken from triplicate runs. <sup>b</sup>  $\pm$ Uncertainties refer to standard deviation.

The solubilities (concentrations) of quinizarin, disperse red 9, and disperse blue 14 were analyzed at their maximum absorbance at 481, 503, and 643 nm, respectively, using a spectrophotometric method. The calibration curve was obtained with twelve standard solutions, over a composition range of ( $8.0 \times 10^{-7}$  to  $2.4 \times 10^{-4}$ ) mol·L<sup>-1</sup>, of ( $7.0 \times 10^{-6}$  to  $3.5 \times 10^{-4}$ ) mol·L<sup>-1</sup> and of ( $2.3 \times 10^{-6}$  to  $1.4 \times 10^{-4}$ ) mol·L<sup>-1</sup> of quinizarin, disperse red 9, and disperse blue 14, respectively, dissolved in an appropriate organic solvent (e.g., methanol).

Three replicates were performed at each experimental condition and the solubility obtained is the average of these results. The uncertainty of the solubility measurements for each isotherm was (4 to 6) %.

### 3. RESULTS AND DISCUSSION

**3.1. Experimental Data.** The experimental solubility data obtained in this study for the three dyes are summarized in

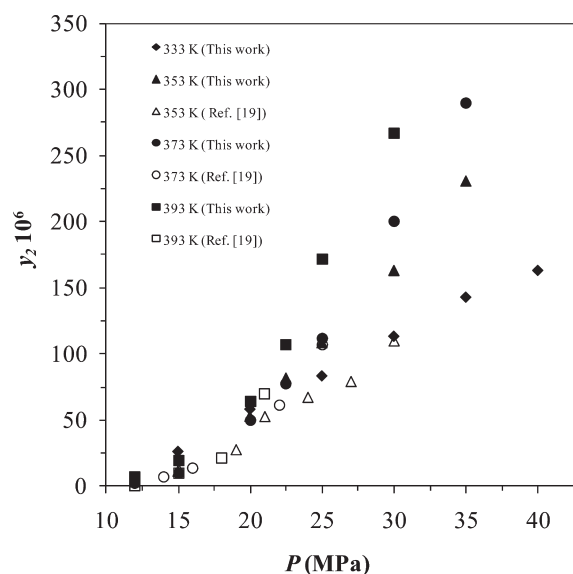


**Figure 1.** Comparison of experimental solubility of quinizarin in SC-CO<sub>2</sub> ( $y_2$ ) vs pressure at different temperatures with literature data.

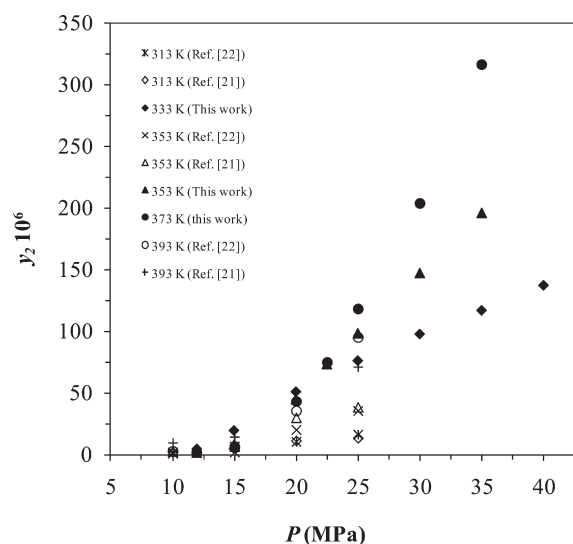


**Figure 2.** Comparison of experimental solubility of red 9 in SC-CO<sub>2</sub> ( $y_2$ ) vs pressure at different temperatures with literature data.

Table 2 and a comparison with those, published in the literature, is presented in Figures 1–3.

The solubility of blue 14 is 1 order of magnitude lower than that of the other two dyes. However, the solubility behavior of the three dyes is similar with a crossover of the respective isotherms at about 20 MPa. Below this pressure the solubility decreases with increasing temperature, whereas an opposite trend is observed at pressures higher than the crossover pressure. The existence of a crossover pressure in solid-SC fluid systems is a result of the following: (i) at constant pressure, below the crossover pressure, the solubility of the dyes decreases as the density of CO<sub>2</sub> decreases with increasing temperature, which means that the temperature enhancement of the density is more important than the temperature enhancement of the vapor pressure of the dyes and (ii) at constant pressure, above the crossover pressure, the solubility of the dyes increases with

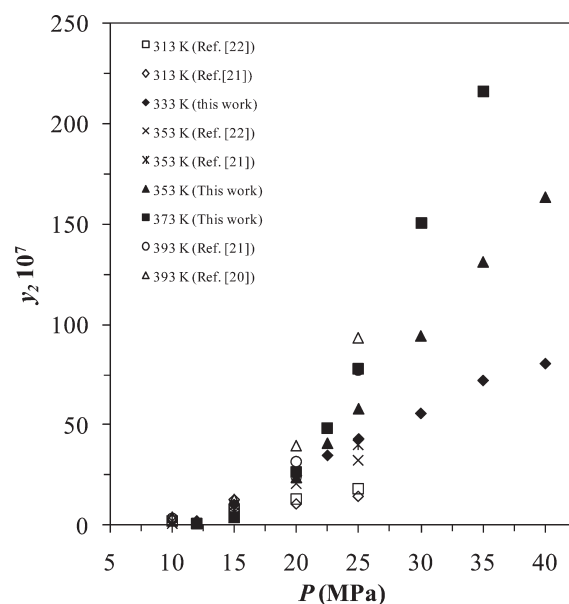


**Figure 3.** Comparison of experimental solubility of blue 14 in SC-CO<sub>2</sub> ( $y_2$ ) vs pressure at different temperatures with literature data.

**Table 3.** Parameters of the Chrastil Equation ( $\ln y_2 = k \ln \rho + s/T + t$ ), for the Dyes + CO<sub>2</sub> Binary Systems, Number of Data Points ( $N$ ), and Average Absolute Relative Deviations (AARD %)

compound	$t$	$k$	$s(K)$	$N$	AARD %
quinizarin	−21.06	4.30	−5709.0	28	14.7
red 9	−25.00	4.94	−5814.8	21	5.7
blue 14	−26.90	5.20	−6737.2	23	7.5

increasing temperature because of the growing diffusion power of the solute.

Figure 1 shows a comparison of each isotherm of the present work with those from the literature for quinizarin.<sup>19</sup> The solubility trend observed is particularly consistent with that observed by Ferri et al.<sup>19</sup> and both data are in a good agreement, particularly for  $T = (333.2 \text{ and } 353.2) \text{ K}$ . However, for  $T = 393.2 \text{ K}$ , at lower values of the pressure, we report higher solubility than Ferri et al.<sup>19</sup> Comparison with the data of Shamsipur et al.<sup>20</sup> shows that the solubility of quinizarin at  $T = (308\text{--}348) \text{ K}$  is in a good agreement over a similar range of temperatures.

Ferri et al.<sup>19</sup> claim that the use of a bypass line can be considered a good variation of the “traditional” flow methodology. Our equipment is designed differently: the volumes of the connection lines and the expansion valve are very low which guarantee a low accumulation of the solid inside them and we use a recovery system with at least three filters in one tube, which gives a better guarantee of a total recovery of the dyes.

Figure 2 shows a comparison of each solubility isotherm of the present study with those from the literature for red 9.<sup>21,22</sup> Over the low pressure ranges (up to 20 MPa) our data are in a good agreement with those previous reported by,<sup>21,22</sup> but differ at higher pressures.

Figure 3 is a display of the comparison of each isotherm from the present study with these in the literature for blue 14.<sup>21,22</sup> Our

**Table 4.** Total Heat of Reaction, Heat of Vaporization, and Solvation Calculated in This Study for the Three Dyes<sup>a</sup>

compound	$\Delta H_{\text{total}}^b$ (kJ mol <sup>-1</sup> )	$\Delta H_{\text{total}}^c$ (kJ mol <sup>-1</sup> )	$\Delta H_{\text{vap}}^d$ (kJ mol <sup>-1</sup> )	$\Delta H_{\text{sol}}^e$ (kJ mol <sup>-1</sup> )
quinizarin	47.46	53.80	63.64	13.01
quinizarin <sup>14</sup>	53.77	53.51	63.90	10.26
red 9	48.34	58.53	67.66	14.23
red 9 <sup>14</sup>	53.79	71.20	84.95	21.15
blue 14	56.01	61.55	74.05	15.27
blue 14 <sup>14</sup>	47.32	58.62	72.37	19.40

<sup>a</sup> Comparison with the results available in the literature. <sup>14</sup> <sup>b</sup> Obtained from Chrastil model. <sup>c</sup> Obtained from K–J model. <sup>d</sup> Obtained from Bartle model.

<sup>e</sup> Obtained from the difference between the  $\Delta H_{\text{vap}}^c$  and  $(\Delta H_{\text{total}}^a + \Delta H_{\text{total}}^b)/2$ .

results for the isotherm of 353.2 K are in a good agreement with those in the literature up to 20 MPa. Above the crossover pressure point our solubility values are higher than the values reported previously.<sup>21,22</sup> Gordillo et al.<sup>12,23</sup> also report experimental solubilities of blue 14 in SC CO<sub>2</sub> up to 35 MPa. Although they do not give numerical values for the solubility of the dye, still it is possible to ascertain that their data are in agreement with those of Joung et al.<sup>21,22</sup> and are lower than ours at higher pressures.

Our flow through apparatus was tested by measuring the solubility of naphthalene in supercritical CO<sub>2</sub> at  $T = (308.2 \text{ and } 318.2) \text{ K}$  at two pressures values, (11 and 30) MPa. The solubilities of naphthalene measured by us agreed within 4% with those of Tsekanskaya et al.<sup>31</sup> often used as a standard for comparison in the literature.

**3.2. Experimental Solubility Data Correlation.** The applicability, effectiveness, and efficiency of different models to correlate the experimental solubility data obtained in the present study was investigated using four density-based correlations (Chrastil, Bartle, Mendez–Santiago–Teja and Kumar and Johnson) and the SRK CEoS with classical van der Waals mixing and combining rules.

**3.2.1. Semi-empirical Density-Based Equations Models.** The application of even simple EoSs, like the CEoS, to correlate the solubility of dyes in SC CO<sub>2</sub> requires fitting of the model parameters and knowledge of the pure dyes properties. Usually these properties are not available and hence have to be estimated applying different methods. With the view to avoid these difficulties, many authors employ semiempirical models. Often only three parameters for a compound are needed to predict its solubility at various pressures and temperatures.

For the three dyes examined, each model parameters were obtained by minimizing the absolute average deviation (AARD) between the solubility values obtained experimentally,  $y_i^{\text{exp}}$ , and those correlated by the model,  $y_i^{\text{calc}}$ , according to the following:

$$\text{AARD} = \left( \frac{100}{N} \right) \left( \sum_{i=1}^N \frac{|y_i^{\text{exp}} - y_i^{\text{calc}}|}{y_i^{\text{exp}}} \right) \quad (1)$$

where  $N$  is the number of data points.

The application of the four density-based equations to correlate the solubility of the dyes proved to be successful, and the results obtained are improved in comparison to those obtained previously for the same systems.<sup>14</sup> Among the four models, the Chrastil equation gave the best fit to the solubility of all three dyes. Even for Blue 14, which has a lower solubility in SC CO<sub>2</sub>, the AARD is only 7.5%.

In Table 3, the values of the parameters of Chrastil equation are reported. One can see the increase of the complexity of

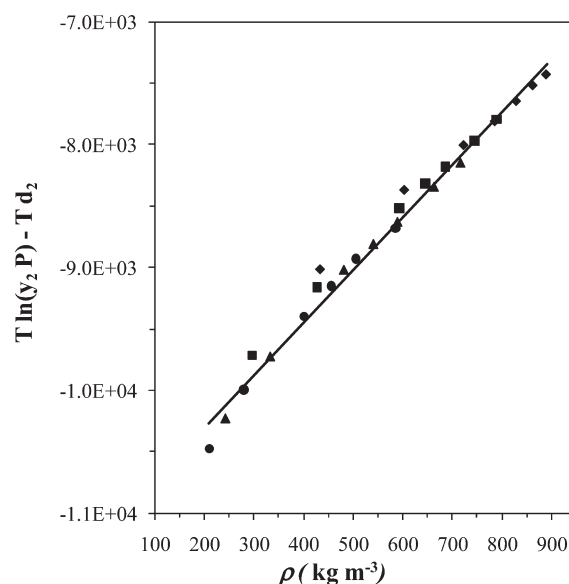


**Figure 4.** Solubility of Quinizarin in SC–CO<sub>2</sub>. Symbols represent experimental solubility; Lines - the solubility correlation using the Méndez-Santiago and Teja equation (—), (◆) 333.2, (▲) 353.2, (■) 373.2, and (●) 393.2 K.

solute–solvent interaction demonstrated by the change in the values of the association parameter  $k$  of the Chrastil equation;  $k$  is increasing from 4.30 (carbon dioxide + quinizarin) to 4.94 (carbon dioxide + red 9) and finally to 5.20 (carbon dioxide + blue 14).

Furthermore, as is well-known,<sup>14</sup> the respective coefficients of the Chrastil and Kumar and Johnston equations can be related to the total heat of reaction ( $\Delta H_{\text{total}}$ ), while the heat of vaporization of the dye, ( $\Delta H_{\text{vap}}$ ), can be estimated from the coefficients of the Bartle model.

The  $\Delta H_{\text{total}}$ ,  $\Delta H_{\text{vap}}$ , and the heat of solvation ( $\Delta H_{\text{sol}}$ ) were determined from the correlation results obtained and are presented in Table 4. For red 9, the deviations between our results and those published previously<sup>14</sup> are high. However, the values of the total heat of reaction, calculated applying either the Chrastil equation or the Kumar and Johnston model are in a better agreement with each other than the corresponding results from the literature.<sup>14</sup>

Finally, as stated by Méndez-Santiago and Teja<sup>26</sup> their model can be used to test the consistency of the solubility data measured. Thus, the experimental data are consistent, if all isotherms collapse to a single line on a graph of  $T \ln(y_2 P) - T d_2$  versus density of supercritical fluid,  $\rho$ . Figure 4 shows that our data for quinizarin obey this criterion.



**Table 5. Quinizarin, Red 9, and Blue 14 Pure Component Properties**

	quinizarin	red 9	blue 14
$p_c/\text{MPa}$	4.14	2.85	2.54
$T_c/\text{K}$	1007.76	750.95	812.35
$p/\text{MPa}$ (triple point)	$5.90 \times 10^{-5}$	$3.37 \times 10^{-5}$	$1.63 \times 10^{-5}$
$V^S/\text{m}^3 \text{ mol}^{-1}$	$1.740 \times 10^{-4}$	$1.81 \times 10^{-4}$	$2.034 \times 10^{-4}$
$V^{\text{SCL}}/\text{m}^3 \text{ mol}^{-1}$	$1.998 \times 10^{-4}$	$2.070 \times 10^{-4}$	$2.319 \times 10^{-4}$
$\Delta H_{\text{fus}}/\text{J mol}^{-1}$	24189 <sup>a</sup>	28750	31012
$T_m/\text{K}$	472.71 <sup>b</sup>	444.2 <sup>b</sup>	494.15 <sup>b</sup>
$P_s^{\text{subl}}/\text{MPa}$ at $T = 333.2 \text{ K}$	$4.41 \times 10^{-9}$	$1.05 \times 10^{-8}$	$1.91 \times 10^{-10}$
$P_s^{\text{subl}}/\text{MPa}$ at $T = 353.2 \text{ K}$	$2.88 \times 10^{-8}$	$1.10 \times 10^{-7}$	$2.05 \times 10^{-9}$
$P_s^{\text{subl}}/\text{MPa}$ at $T = 373.2 \text{ K}$	$1.44 \times 10^{-7}$	$9.00 \times 10^{-7}$	$1.71 \times 10^{-8}$
$P_s^{\text{subl}}/\text{MPa}$ at $T = 393.2 \text{ K}$	$6.05 \times 10^{-7}$	-	-

<sup>a</sup> Ref 34. <sup>b</sup> Ref 32.

**3.2.2. Equation of State Method: Thermodynamic Framework.** To compute the solubility (mole fraction) of a solid solute in the fluid phase at a specified temperature, pressure, and overall composition an appropriate thermodynamic model is required.

The standard formulation of this problem is based on the equilibrium condition for the solute; that is, assuming an EoS model for the fluid phase and denoting by the superscript “S” the solid solute and by the superscript F the fluid phase:

$$f^S(T, P) = f^F(T, P, \mathbf{y}, V) \quad (2)$$

where  $f^S$  is the fugacity of the solute in the pure solid phase,  $f^F$  is fugacity of the solute in the fluid-phase solution,  $\mathbf{y} = (y_1, y_2, \dots, y_{N_c})^T$  is the vector of fluid-phase mole fractions, and  $V$  is the molar volume of the fluid from the EoS model. Additional relationships that must be satisfied are the summation to one of the fluid-phase mole fractions.

The more common approach to the solution of the above problem is to take a popular EoS and use it directly in solid–fluid equilibrium calculations by introducing a solid-phase fugacity function defined in terms of a fluid–phase reference state. In this study we implement the fugacity of a hypothetical subcooled liquid phase, as the reference of the solid phase fugacity. Thus, the solid–phase fugacity function, for a pure solute solid phase at temperature  $T$  and pressure  $P$ , defined in terms of a hypothetical liquid–phase fugacity as a reference state, disregarding the change in specific heat, is given as<sup>32</sup>

$$f^S = f^{\text{SCL}}(P, T) \exp \left( \int_{P_s^{\text{subl}}}^P \frac{V^S - V^{\text{SCL}}}{RT} dP + \frac{\Delta H_{\text{fus}}}{R} \left( \frac{1}{T_m} - \frac{1}{T} \right) \right) \quad (3)$$

Assuming that there are no solid–solid phase transitions and provided the solid specific volume at the subcooled liquid state  $V^{\text{SCL}}$  is only weakly dependent on pressure, eq 3 can be written as follows:

$$f^S = f^{\text{SCL}}(P, T) \exp \left( \frac{(V^S - V^{\text{SCL}})(P - P_s^{\text{subl}}(T))}{RT} + \frac{\Delta H_{\text{fus}}}{R} \left( \frac{1}{T_m} - \frac{1}{T} \right) \right) \quad (4)$$

In eq 4,  $f^{\text{SCL}}$  is the fugacity of the pure subcooled liquid,  $\Delta H_{\text{fus}}$  is the enthalpy of fusion,  $\Delta V_{\text{fus}} = V^S - V^{\text{SCL}}$  is the change in

**Table 6. Binary Interaction Parameters ( $k_{ij}$ ) and AARD for the Systems Quinizarin + CO<sub>2</sub>, Red 9 + CO<sub>2</sub> and Blue 14 + CO<sub>2</sub> at the Temperatures of the Experiment**

$T/\text{K}$	quinizarin + CO <sub>2</sub>		red 9 + CO <sub>2</sub>		blue 14 + CO <sub>2</sub>	
	$k_{ij}$	AARD %	$k_{ij}$	AARD %	$k_{ij}$	AARD %
333.2	0.1682	6.86	0.1512	3.58	0.1453	6.95
353.2	0.1417	4.63	0.1403	9.73	0.1582	5.38
373.2	0.1265	3.85	0.1320	11.01	0.1710	4.91
393.2	0.1108	5.28				

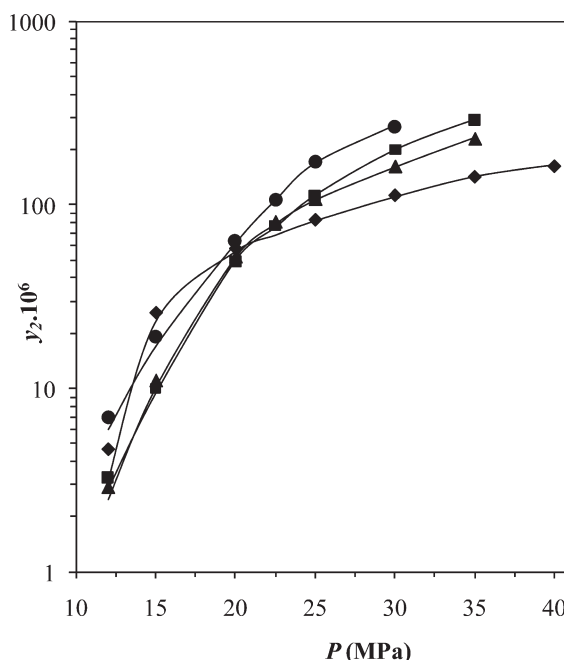


**Figure 5.** Solubility of quinizarin in SC–CO<sub>2</sub>. Symbols represent experimental solubility; lines, the solubility correlation using the SRK EoS (—), (♦) 333.2, (▲) 353.2, (■) 373.2, and (●) 393.2 K.

volume, all taken for the solute at its triple point. The fugacity of the pure subcooled liquid  $f^{\text{SCL}}$  is calculated from an EoS (in our case SRK EoS). The values of  $V^{\text{SCL}}$  are also evaluated by the EoS assuming that the volume is independent of pressure and temperature and equal to the value at the normal melting point.

**3.2.3. Pure Component Properties Estimation.** To calculate the fugacity of a pure solid solute according to eq 4, the following data are required: its fusion properties (enthalpy of fusion ( $\Delta H_{\text{fus}}$ ), melting temperature ( $T_m$ ),  $\Delta V_{\text{fus}}$  and sublimation pressure ( $P_s^{\text{subl}}$ ), and its critical parameters ( $T_c$  and  $P_c$ ). Generally, most of these properties are either not available experimentally or are even hypothetical and hence have to be predicted applying different estimation and group-contribution methods. Thus, this may introduce errors in the correlation results, or may lead to varying values for each model's parameters.<sup>33</sup>

For the three dyes discussed in our study the experimental data presented in the literature are extremely scarce and include only the melting temperatures<sup>33,34</sup> and the enthalpy of fusion for quinizarin, which was obtained by DSC analysis.<sup>35</sup> The other properties required are not available. To estimate them we followed the algorithm discussed in detail by Fornari et al.<sup>36</sup>

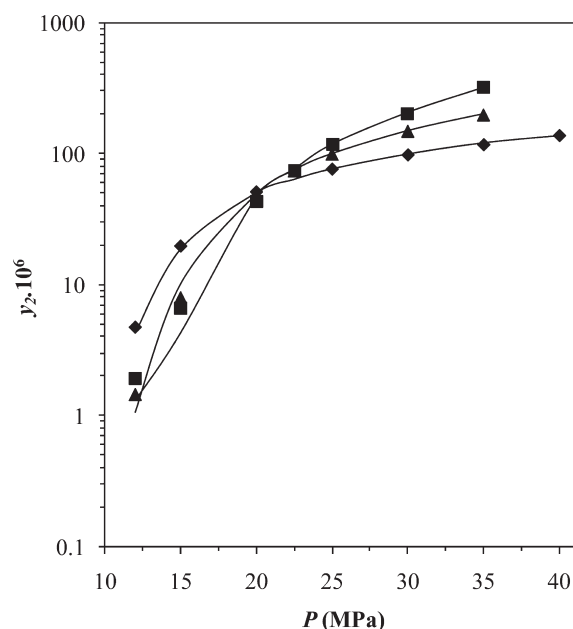


**Figure 6.** Solubility of red 9 in SC-CO<sub>2</sub>. Symbols represent experimental solubility; lines, solubility correlation using the SRK EoS (—), (♦) 333.2, (▲) 353.2, and (■) 373.2 K.

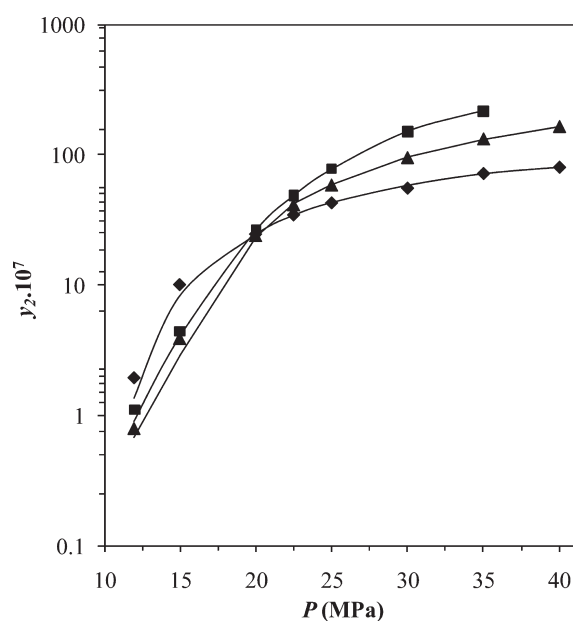


**Figure 7.** Solubility of blue 14 in SC-CO<sub>2</sub>. Symbols represent experimental solubility; lines, solubility correlation using the SRK EoS (—), (♦) 333.2, (▲) 353.2, and (■) 373.2 K.

Herewith we mark only the relevant main steps: The enthalpies of fusion were estimated applying the method of Jain et al.<sup>37</sup> The sublimation pressures at the temperatures of interest to the experiment were calculated from the Clapeyron equation, applying the data from the melting properties of the three dyes; The solid molar volumes were estimated applying the method of Bondi.<sup>38</sup> The critical parameters were estimated applying the methods suggested by Wakeham et al.<sup>39</sup> and Brauner et al.<sup>40</sup> Finally, the fugacity of the pure solutes in the subcooled liquid phase, the triple point pressure and  $V^{SCL}$  were all calculated from

the EoS. The pure component properties of the three dyes used in our work are summarized in Table 5.

The thermodynamic model applied was the SRK CEoS with the one-fluid van der Waals mixing rule with one parameter (VdW1).<sup>28</sup> The unlike-pair interaction parameters,  $k_{ij}$ , were correlated from the experimental data measured in this study. As pointed out previously, the  $k_{ij}$  values often incorporate the possible errors in the estimated thermophysical properties of the pure solid solutes. Therefore, some investigators use as optimization parameters both the solid solute sublimation pressure and the interaction parameter as a constant independent of temperature.<sup>12,13</sup> Nevertheless, such approach does not necessarily guarantee low deviations between correlated results and experimental data, while, in our view, increases to some extent the complexity of the iterative procedures resulting in their convergence.

The values of the interaction parameters determined for the three binary systems (dye+SC CO<sub>2</sub>) as well as the AARD between the solubility values measured experimentally,  $y_i^{exp}$ , and those correlated by the EoS model,  $y_i^{calc}$  are presented in Table 6.

The agreement between the  $y_i^{exp}$  and  $y_i^{calc}$  for the three dyes is acceptable; moreover it improves considerably after the crossover into higher pressure for the respective compound, where the experimental conditions are far from CO<sub>2</sub> critical point, and where cubic EoSs perform better (Figures 5–7).

#### 4. CONCLUSIONS

In this work, the solid solubilities in supercritical CO<sub>2</sub> of three important disperse dyes, namely, quinizarin, red 9, and blue 14 are measured for the first time in a consistent way at a temperature range from (333.2 to 393.2) K and at pressures from (12.0 to 40.0) MPa. Furthermore, solubility values at different temperatures and at pressures higher than 35.5 MPa for quinizarin<sup>20</sup> and blue 14,<sup>12,23</sup> and higher than 25.0 MPa for red 9 have not been previously reported in the literature. The solubilities of the dyes decrease in the order quinizarin > red 9 > blue 14.

Among the four semiempirical density-based models applied to correlate the dyes' solubility the Chrastil equation gave the best results, with an overall AARD of 9.3%, which is within the experimental uncertainty. In the particular cases studied the performance of the Mendez-Santiago–Teja model is inferior to the Chrastil one, but the former can be used with confidence to test the consistency of the experimental data.

The SRK EoS with the one-fluid van der Waals mixing rule was shown to be able to provide a good correlation of the solubility of the three dyes in SC CO<sub>2</sub>. The thermophysical parameters of the pure solid solutes, required by the modeling, for which there were no data available were estimated and reported.

#### AUTHOR INFORMATION

##### Corresponding Author

\*Fax: (+351) 218317151. E-mail: jcoelho@deq.isel.ipl.pt.

#### REFERENCES

- (1) Montero, G. A.; Smith, C. B.; Hendrix, W. A.; Butcher, D. L. Supercritical fluid technology in textile processing: An Overview. *Ind. Eng. Chem. Res.* **2000**, 39 (12), 4806–4812.
- (2) Guzel, B.; Akgerman, A. Mordant dyeing of wool by supercritical processing. *J. Supercrit. Fluids* **2000**, 18 (3), 247–252.

- (3) Sicardi, S.; Manna, L.; Banchemo, M. Diffusion of disperse dyes in PET films during impregnation with a supercritical fluid. *J. Supercrit. Fluids* **2000**, *17* (2), 187–194.
- (4) Banchemo, M.; Manna, L.; Ferri, A. Effect of the addition of a modifier in the supercritical dyeing of polyester. *Color. Technol.* **2010**, *126*, 171–175.
- (5) Ozcan, A. S.; Clifford, A. A.; Bartle, K. D.; Lewis, D. M. Solubility of disperse dyes in supercritical carbon dioxide. *J. Chem. Eng. Data* **1997**, *42*, 590–599.
- (6) Tuma, D.; Schneider, G. M. High-pressure solubility of disperse dyes in near and supercritical fluids: measurements up 100 MPa by a static method. *J. Supercrit. Fluids* **1998**, *13*, 37–42.
- (7) Wagner, B.; Kautz, C. B.; Schneider, G. M. Investigations on the solubility of anthraquinone dyes in supercritical carbon dioxide by a flow method. *Fluid Phase Equilib.* **1999**, *158–160*, 707–712.
- (8) Guzel, B.; Akgerman, A. Solubility of disperse and mordant dyes in Supercritical CO<sub>2</sub>. *J. Chem. Eng. Data* **1999**, *44*, 83–85.
- (9) Tuma, D.; Wagner, B.; Schneider, G. M. Comparative solubility investigations of anthraquinone disperse dyes in near- and supercritical fluids. *Fluid Phase Equilib.* **2001**, *182*, 133–143.
- (10) Lin, H.; Liu, C.; Cheng, C.; Chen, Y.; Lee, M. Solubilities of disperse dyes of blue 79, red 153, and yellow 119 in supercritical carbon dioxide. *J. Supercrit. Fluids* **2001**, *21*, 1–9.
- (11) Lee, J. W.; Park, M. W.; Bae, H. K. Measurement and correlation of dye solubility in supercritical carbon dioxide. *Fluid Phase Equilib.* **2001**, *179*, 378–394.
- (12) Gordillo, M. D.; Pereyra, C.; Martinez de la Ossa, E. J. Measurement and correlation of solubility of Disperse Blue 14 in supercritical carbon dioxide. *J. Supercrit. Fluids* **2003**, *27*, 31–33.
- (13) Tamura, K.; Shinoda, T. Binary and Ternary Solubilities of disperse dyes and their blend in supercritical carbon dioxide. *Fluid Phase Equilib.* **2004**, *219*, 25–32.
- (14) Huang, Z.; Guo, Y.; Sun, G.; Chiew, Y.; Kawi, S. Representing dyestuff solubility in supercritical carbon dioxide with several density-based correlations. *Fluid Phase Equilib.* **2005**, *236*, 136–145.
- (15) Banchemo, M.; Ferri, A.; Manna, L.; Sicardi, S. Solubility of disperse dyes in Supercritical carbon dioxide and ethanol. *Fluid Phase Equilib.* **2006**, *243*, 107–114.
- (16) Ozcan, A. S.; Ozcan, A. Measurements and correlation of solubility of Acid Red 57 in supercritical carbon dioxide by ion-pairing with hexadecyltrimethylammonium bromide. *J. Supercrit. Fluids* **2006**, *37*, 23–28.
- (17) Tabaraki, R.; Khayamian, T.; Ensafi, A. A. Solubility prediction of 21 azo dyes in supercritical carbon dioxide using wavelet neural network. *Dyes Pigm.* **2007**, *73*, 230–238.
- (18) Tsai, C. C.; Lin, H. M.; Lee, M.-J. Solubility of 1,5-Diamino-bromo-4,8-dihydroxyanthraquinone in supercritical carbon dioxide with or without cosolvent. *J. Chem. Eng. Data* **2009**, *54*, 1442–1446.
- (19) Ferri, A.; Banchemo, M.; Manna, L.; Sicardi, S. An experimental technique for measuring high solubilities of dyes in supercritical carbon dioxide. *J. Supercrit. Fluids* **2004**, *30*, 41–49.
- (20) Shamsipur, M.; Fasihi, J.; Khanchic, A.; Yaminib, Y.; Valinezhadd, A.; Sharghie, H. Solubilities of some 9,10-anthraquinone derivatives in supercritical carbon dioxide: A cubic equation of state correlation. *J. Supercrit. Fluids* **2008**, *47*, 154–160.
- (21) Joung, S. N.; Shin, H. Y.; Park, Y. H.; Yoo, K. Measurement and correlation of solubility of disperse anthraquinone and azo dyes in supercritical carbon dioxide. *Korean J. Chem. Eng. Data* **1998**, *15* (1), 78–84.
- (22) Joung, S. N.; Yoo, K. Solubility of disperse anthraquinone and azo dyes in supercritical carbon dioxide at 313.15 to 393.15K and from 10 to 25 MPa. *J. Chem. Eng. Data* **1998**, *43*, 9–12.
- (23) Gordillo, M. D.; Pereyra, C.; Martinez de la Ossa, E. J. Solubility estimations for disperse Blue 14 in supercritical carbon dioxide. *Dyes Pigm.* **2005**, *67*, 167–173.
- (24) Chrastil, J. Solubility of solids and liquids in supercritical gases. *J. Phys. Chem.* **1982**, *86*, 3016–3021.
- (25) Bartle, K. D.; Clifford, A. A.; Jafar, S. A.; Shilstone, G. F. Solubilities of solids and liquids of low volatility in supercritical carbon dioxide. *J. Phys. Chem. Ref. Data* **1991**, *20*, 713–756.
- (26) Mendez-Santiago, J.; Teja, A. S. The solubility of solids in supercritical fluids. *Fluid Phase Equilib.* **1990**, *158–160*, 501–510.
- (27) Kumar, S. K.; Johnston, K. P. Modelling solubility of solids in supercritical fluids with density as the independent variable. *J. Supercrit. Fluids* **1988**, *1*, 15–22.
- (28) Soave, G. Equilibrium Constants from a Modified Redlich-Kwong Equation of State. *Chem. Eng. Sci.* **1972**, *27*, 1197–1203.
- (29) Coelho, J. P.; Bernotaityte, K.; Miraldes, M. A.; Mendonça, A. F.; Stateva, R. P. Solubility of ethanamide and 2-propenamide in supercritical carbon dioxide. Measurements and correlation. *J. Chem. Eng. Data* **2009**, *54*, 2546–2549.
- (30) Marques A. J. V.; Coelho J. A. P. Determination off at contents with supercritical CO<sub>2</sub> extraction in two commercial powder chocolate products: Comparison with NP-1719. *J. Food Process Eng.* Accepted for publication September 14, **2009**; doi: 10.1111/j.1745-4530.2009.00543.x.
- (31) Tsekhanskaya, Y. V.; Iomtev, M. B.; Mushkina, E. V. Solubility of naphthalene in ethylene and carbon dioxide under pressure. *Russ. J. Phys. Chem.* **1964**, *38*, 1173–1176.
- (32) Prausnitz, J. M.; Lichtenthaler, R. N.; Azevedo, E. G. *Molecular Thermodynamics of Fluid-Phase Equilibria*; Prentice Hall: Englewood Cliffs, NJ, 1999.
- (33) Coimbra, P.; Gil, M. H.; Heron, B. M.; Sousa, H. C. Solubility of a spiroindolinonaphthoxazine photochromic dye in supercritical carbon dioxide: Experimental determination and correlation. *Fluid Phase Equilib.* **2005**, *238*, 120–128.
- (34) Thermophysical Properties of Fluid System, National Institute of Standards and Technology, Available online: <http://webbook.nist.gov/chemistry/name-ser.html> (accessed in November 2009)
- (35) Ferri, A.; Banchemo, M.; Mauna, L.; Sicardi, S. A new correlation of solubilities of azoic compounds and anthraquinone derivatives in SC CO<sub>2</sub>. *J. Supercrit. Fluids* **2004**, *32*, 27–35.
- (36) Fornari, T.; Chafer, A.; Stateva, R. P.; Reglero, G. A. New development in the application of the group contribution associating equation of state to model solid solubilities of phenolic compounds in SC–CO<sub>2</sub>. *Ind. Eng. Chem. Res.* **2005**, *44*, 8147–8156.
- (37) Jain, A.; Yang, G.; Yalkowsky, S. H. Estimation of melting points of organic compounds. *Ind. Eng. Chem. Res.* **2004**, *43*, 7618–7621.
- (38) Bondi, A. van der Waals Volumes and Radii. *J. Phys. Chem.* **1964**, *68*, 441–451.
- (39) Wakeham, W. A.; Cholakov, G. St.; Stateva, R. P. Liquid density and critical properties of hydrocarbons estimated from molecular structure. *J. Chem. Eng. Data* **2002**, *47*, 559–570.
- (40) Brauner, N.; Stateva, R. P.; Cholakov, G. St.; Shacham, M. Structurally “targeted” quantitative structure-property relationship method for property prediction. *Ind. Eng. Chem. Res.* **2006**, *45*, 8430–8437.